State Estimation for Mitigating Positioning Errors in V2V Networks Employing Dual Beamforming

Nivetha Kanthasamy* Raghvendra V. Cowlagi† Alexander M. Wyglinski*

†Department of Electrical and Computer Engineering, Worcester Polytechnic Institute, Worcester, MA
*Department of Mechanical Engineering, Worcester Polytechnic Institute, Worcester, MA
{nkanthasamy, rvcowlagi, alexw}@wpi.edu

***Abstract*— In this paper, we present a novel approach for mitigating positioning errors in vehicle-to-vehicle (V2V) networking environments where digital beamforming is conducted at both transmitters and receivers. Location information of all transmitters and receivers in V2V networks performing beamforming is essential in order to ensure reliable link quality. However, there exists several sources of error where this location information can be corrupted or out-of-date. By leveraging the proposed approach in this paper employing state estimation, these errors can be mitigated, thus providing more accurate location information relative to V2V networking architectures that do not employ techniques to help mitigate potential sources of location error. Simulation results show a 99% improvement of the proposed approach relative to V2V beamformiong architectures that do not account for location errors.**

I. Introduction

Wireless connectivity is a key technology for enabling the reliable operation of self-driving cars in complex and challenging environments such as traffic intersections and multi-lane roads. Until the writing of this paper, most information sources used by self-driving cars to support their real-time situational awareness have been obtained from *line-of-sight* (LOS) sensors such as Light Detection and Ranging (LiDAR) [1], Radio Detection and Ranging (RADAR) [2], and vision systems [3]. Combining these information sources with geographical databases of various driving environments [4] [5], self-driving cars have performed reasonably well with respect to traversing public streets and highways in ideal situations without substantial challenges to the real-time control algorithms managing the operations of the vehicles [6].

Despite the achievements of current self-driving car technology, there is still much work that needs to be done in order to make these vehicles reliable and safe across a plethora of operating conditions. Although LOS sensors excel at gathering information about the surrounding driving environment to provide the self-driving car with adequate situational awareness, this environmental perception only extends approximately a hundred meters, which is insufficient for complex driving environments (*e.g.*, traffic intersections, multi-lane highways) or challenging conditions (*e.g.*, inclement weather, tunnels). Consequently, research and development efforts are currrently underway to explore wireless connectivity as a *non-line-of-sight* (NLOS) source of environmental information that can be used by the self-driving car to support safe and reliable operation in these conditions [7] [8]. In particular, efforts are being pursued to devise *vehicle-to-vehicle* (V2V) networking, where individual vehicles communicate directly with each other without the need for a base station, access point, or road-side unit [9] [10].

To ensure that all vehicles on the road, both human-operated and self-driving, obtain real-time access to wireless channel bandwidth while operating, techniques are needed to ensure sufficient spectral capacity for potentially hundreds of vehicles that could be communicating simultaneously. Although approaches such as *vehicular dynamic spectrum access* (VDSA) [11] have shown potential to allieivate the issue of vehicular spectrum scarcity, there still exists the issue of sufficient wireless access for V2V networks in dense traffic conditions [12]. Consequently, *digital beamforming* for V2V networking has been proposed in order to increase capacity in these environments [13]. By leveraging digital beamforming between transmitting and receiving vehicles within a V2V communications link, wireless spectrum is only being used within a specific spatial direction across a specific frequency channel at a given time, thus minimizing out-of-band (OOB) interference to other V2V wireless links while simultaneously minimizing emissions from other wireless transmissions. However, to enable functional V2V wireless links employing digital beamforming at both ends, accurate real-time position information of both transmit and receive vehicles needs to be known, which can be challenging in highly dynamic and mobile environments.

In this paper, we propose a novel approach for mitigating position errors associated with V2V wireless links where both transmitter and receiver vehicles are employing digital beamforming. Although it is expected that most vehicles, especially self-driving cars, will possess access to geographical databases, global navigation satellite systems (GNSS), and basic safety messages (BSMs) to determine their location in real-time, there is potential for location errors to occur that can signficantly impact the performance of the dual-beamforming and negatively impact the quality of the V2V wireless link. GNSS errors and latency due to location updating could result in the transmitter and receiver digital beamforming being pointed at directions other than the target vehicles. Consequently, leveraging state information

978-1-5386-6358-5/18/$31.00 ©2018 IEEE

of the vehicles and their driving paths can help mitigate these errors, thus yielding a performance improvement when compared to V2V dual beamforming implementations where these measures are not implemented. Without loss of generality, we explore in this work how dual beamforming V2V wireless links operate in complex driving conditions for two vehicles; the results can be readily extended to environments possessing multiple vehicles operating simultaneously.

The rest of this paper is organized as follows: Section II presents the vehicle dynamics problem formulation for this work across various operating conditions. Section III defines the proposed state estimation process to be employed in these environments from which this information will be used to mitigate the location error introduced to the dual beamforming V2V communication link. Section IV presents several simulation results highlighting the performance improvements of employing the proposed state estimation approach when compared to scenarios where location information of every vehicle is perfectly known and when the dual beamforming V2V wireless links are used without the proposed approach. Finally, concluding remarks are presented in Section V.

II. Problem Formulation

For simplicity, we address in this paper situations involving two cars: the ego car and one other vehicle. In what follows, the subscripts "**e**" and "**o**" are used to denote variables associated with the ego vehicle and the other vehicle, respectively.

Let $\mathcal{I}$ be an inertial frame of reference with an attached Cartesian coordinate axes system (see Fig. 1). In what follows, we will also need a moving reference frame $\mathcal{E}$ attached to the ego vehicle, such that a principal Cartesian coordinate axis of $\mathcal{E}$ always points along the ego vehicle's velocity vector, as indicated in Fig. 1.

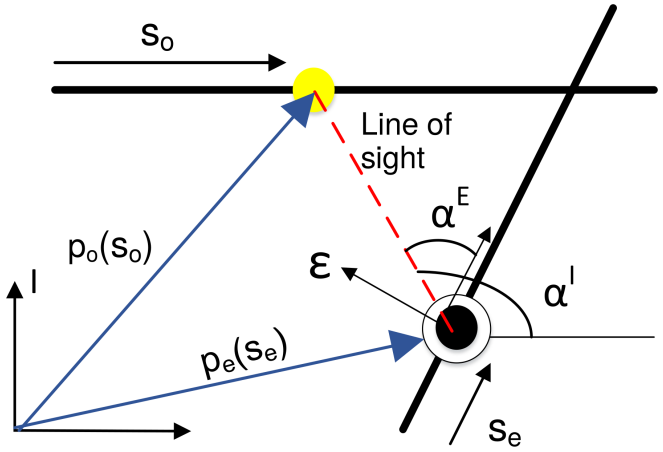

Fig. 1. Illustration of the problem setup. Th ego car is indicated by an encircled black dot, whereas the other car is indicated by a yellow dot.

The geometries of the roads along which the two vehicle travel are assumed to be perfectly known. Specifically, a one-parameter curve defining each road is assumed to be known. This assumption is justified by the abundant availability of accurate electronic maps of roads. We denote by $\mathbf{p}_{\mathrm{e}}(s) = (p_{x,\mathrm{e}}(s), p_{y,\mathrm{e}}(s))$ and $\mathbf{p}_{\mathrm{o}}(s) = (p_{x,\mathrm{o}}(s), p_{y,\mathrm{o}}(s))$ the $\mathcal{I}-$coordinates of each road parameterized by the distance s along the road[1].

With the preceding assumption about road geometry, the location of each car is fully determined by a single parameter, namely the distance traveled along the road. The state of each car is described by its location, denoted by s_{e} and s_{o}, respectively, and by the speed of each var along the road, denoted by v_{e} and v_{o}, respectively. Therefore, the state variables of the cars are $\mathbf{x}_{\mathrm{e}} := (s_{\mathrm{e}}, v_{\mathrm{e}})$ and $\mathbf{x}_{\mathrm{o}} := (s_{\mathrm{o}}, v_{\mathrm{o}})$, respectively.

For each car, we assume the acceleration along the road to be a control input. Whereas this paper does not address autonomous control, this formulation is convenient for future extensions of this work. The accelerations of the cars are denoted by u_{e} and u_{o}, respectively. The state evolution models for the ego and other vehicle are then described by the linear dynamical systems:

$$\dot{\mathbf{x}}_{\mathrm{e}} = A\mathbf{x}_{\mathrm{e}} + Bu_{\mathrm{e}}, \qquad \dot{\mathbf{x}}_{\mathrm{o}} = A\mathbf{x}_{\mathrm{o}} + Bu_{\mathrm{o}},$$

where:

$$A := \begin{bmatrix} 0 & 1 \\ 0 & 0 \end{bmatrix} \qquad B := \begin{bmatrix} 0 \\ 1 \end{bmatrix}. \tag{1}$$

Next, we formulate state evolution and measurement models from the perspective of the ego vehicle. To this end, we assume that the ego vehicle has an onboard localization system that can provide a measurement $\mathbf{y}_{\mathrm{e}}$ of the $\mathcal{I}-$coordinates of the ego vehicle's position and its speed. This assumption is in keeping with standard localization systems that are present on many modern cars, and on all self-driving cars. We also assume that the ego car's acceleration is measured. All of these measurements are noisy. These assumptions lead to the following state evolution and measurement model of the ego vehicle:

$$\dot{\mathbf{x}}_{\mathrm{e}} = A\mathbf{x}_{\mathrm{e}} + B(u_{\mathrm{e}} + \eta_{\mathrm{e}}), \qquad \mathbf{y}_{\mathrm{e}} = h_{\mathrm{e}}(\mathbf{x}_{\mathrm{e}}) + \mathbf{n}_{\mathrm{e}},$$

where η_{e} is the acceleration measurement noise, $h_{\mathrm{e}}(\mathbf{x}_{\mathrm{e}}) := [\mathbf{p}_{\mathrm{e}}(s_{\mathrm{e}}) \quad v_{\mathrm{e}}]^{\mathrm{T}}$, and $\mathbf{n}_{\mathrm{e}}$ is the localization and speed measurement noise. In what follows, we will present a discretized version of this model, where the statistical characteristics of the noise processes will be discussed.

Next, we assume that the other vehicle communicates its position in $\mathcal{I}-$coordinates, its speed, and its acceleration over a V2V link between the two cars. All of these quantities are treated by the ego vehicle as "measurements," and are all noisy. These assumptions lead to the following state evolution and measurement model of the other vehicle as perceived by the ego vehicle:

$$\dot{\mathbf{x}}_{\mathrm{o}} = A\mathbf{x}_{\mathrm{o}} + B(u_{\mathrm{o}} + \eta_{\mathrm{o}}), \qquad \mathbf{y}_{\mathrm{o}} = h_{\mathrm{o}}(\mathbf{x}_{\mathrm{o}}) + \mathbf{n}_{\mathrm{o}}, \tag{2}$$

where η_{o} is the acceleration measurement noise, $h_{\mathrm{o}}(\mathbf{x}_{\mathrm{o}}) := [\mathbf{p}_{\mathrm{o}}(s_{\mathrm{o}}) \quad v_{\mathrm{o}}]^{\mathrm{T}}$, and $\mathbf{n}_{\mathrm{o}}$ is the other vehicle's localization and speed measurement noise.

[1]The "start" of each road defined by $\mathbf{p}_{\mathrm{e}}(0)$ and $\mathbf{p}_{\mathrm{o}}(0)$ is assumed to be prespecified.

A. Model Discretization

The ego car's self-localization system is assumed to update periodically every $\delta t_{\rm e}$ s. The time instants at which data is transmitted over the V2V are denoted $t_{{\rm o},0}, t_{{\rm o},1} \ldots$, which are not assumed to be equally spaced.

Accordingly, we may discretize the preceding state evolution models; because the models are linear, the following discretization is exact [14]:

$$\begin{aligned}
\mathbf{x}_{\rm e}(t_k) &= \Phi_{\delta t}\mathbf{x}_{\rm e}(t_{k-1}) + \Psi_{\delta t}(u_{\rm e}(t_{k-1}) + \eta_{\rm e}(t_{k-1})),\\
\mathbf{x}_{\rm o}(t_k) &= \Phi_{\delta t}\mathbf{x}_{\rm o}(t_{k-1}) + \Psi_{\delta t}(u_{\rm o}(t_{k-1}) + \eta_{\rm o}(t_{k-1})),\\
\mathbf{y}_{\rm e}(t_k) &= h_{\rm e}(\mathbf{x}_{\rm e}(t_k)) + \mathbf{n}_{\rm e}(t_k),\\
\mathbf{y}_{\rm o}(t_k) &= h_{\rm o}(\mathbf{x}_{\rm o}(t_k)) + \mathbf{n}_{\rm o}(t_k),
\end{aligned}$$

where $\delta t := t_k - t_{k-1}$ and:

$$\Phi_{\delta t} := \begin{bmatrix} 1 & \delta t \\ 0 & 1 \end{bmatrix}, \qquad \Psi_{\delta t} := \begin{bmatrix} \delta t/2 \\ 1 \end{bmatrix} \delta t. \tag{3}$$

In this discretized model, we assume that each of the noise terms are independent and identically distributed zero-mean Gaussian random variables with the following statistical characteristics at any time instant t:

$$\begin{aligned}
\mathbf{n}_{\rm e}(t) &\sim \mathcal{N}(\mathbf{0}_{3,1}, R_{\rm e}), \qquad & \mathbf{n}_{\rm o}(t) &\sim \mathcal{N}(\mathbf{0}_{3,1}, R_{\rm o}),\\
\eta_{\rm e}(t) &\sim \mathcal{N}(0, q_{\rm e}), & \eta_{\rm o}(t) &\sim \mathcal{N}(0, q_{\rm o}).
\end{aligned}$$

Here $R_{\rm e}, R_{\rm o}$ are positive definite covariance matrices characterizing ego self-localization and speed measurement error and the other car's localization and speed measurement errors, respectively. Similarly, $q_{\rm e}, q_{\rm o}$ are positive variances characterizing acceleration measurement errors.

III. Proposed Estimation of State and Boresight Angle

After establishing the state evolution and measurement models in the previous section, the estimation of the states of the two car (performed onboard the ego car) follows immediately from linear systems estimation theory [15]. We denote by $\hat{\mathbf{x}}_{\rm e} = (\hat{s}_{\rm e}, \hat{v}_{\rm e})$ and $\hat{\mathbf{x}}_{\rm o} = (\hat{s}_{\rm o}, \hat{v}_{\rm o})$ the estimated states of the ego and other car, respectively.

Let t_k be a time instant at which the $k^{\rm th}$ measurement is available. That is t_k is either a multiple of $\delta t_{\rm e}$ when the ego car localization, speed, and acceleration measurement update is available, or $t_k = t_{{\rm o},n}$ for some integer n, when measurements from the other car are received over the V2V link, or both. Define $\delta t = t_k - t_{k-1}$, *i.e.*, δt is the time step between two successive measurements[2].The available measurements are $\mathbf{y}_{\rm e}(t_k), \mathbf{y}_{\rm o}(t_k)$ and $\tilde{u}_{\rm e}(t_{k-1}) := u_{\rm e}(t_{k-1}) + \eta_{\rm e}(t_{k-1})$ and $\tilde{u}_{\rm o}(t_{k-1}) := u_{\rm o}(t_{k-1}) + \eta_{\rm o}(t_{k-1})$. Note that $u_{\rm e}$ and $u_{\rm o}$ are not directly available. Note also that $\mathbf{y}_{\rm e}(t_k), \mathbf{y}_{\rm o}(t_k)$ may not be both "new" measurements at each t_k : for example if $t_k = t_{{\rm o},n}$ when data over the V2V are received in between two successive updates of the ego car's self-localization, then $\mathbf{y}_{\rm e}(t_k) = \mathbf{y}_{\rm e}(t_{k-1})$.

The following are the standard recursive equations for a discrete-time Kalman filter to update the state estimates at time t_k, using the previous estimates $\hat{\mathbf{x}}_{\rm e}(t_{k-1}), \hat{\mathbf{x}}_{\rm o}(t_{k-1})$ and the estimation error covariance matrices $P_{\rm e}(t_{k-1})$ and $P_{\rm o}(t_{k-1})$:

$$\hat{\mathbf{x}}_{\rm e}^- := \Phi_{\delta t}\hat{\mathbf{x}}_{\rm e}(t_{k-1}) + \Psi_{\delta t}\tilde{u}_{\rm e}(t_{k-1}), \tag{4}$$

$$\hat{\mathbf{x}}_{\rm o}^- := \Phi_{\delta t}\hat{\mathbf{x}}_{\rm o}(t_{k-1}) + \Psi_{\delta t}\tilde{u}_{\rm o}(t_{k-1}), \tag{5}$$

$$P_{\rm e}^- := \Phi_{\delta t}P_{\rm e}(t_{k-1})\Phi_{\delta t}^{\rm T} + \Psi_{\delta t}q_{\rm e}\Psi_{\delta t}^{\rm T}, \tag{6}$$

$$P_{\rm o}^- := \Phi_{\delta t}P_{\rm o}(t_{k-1})\Phi_{\delta t}^{\rm T} + \Psi_{\delta t}q_{\rm o}\Psi_{\delta t}^{\rm T}, \tag{7}$$

$$\hat{\mathbf{x}}_{\rm e}(t_k) = \hat{\mathbf{x}}_{\rm e}^- + K_{\rm e}(\mathbf{y}_{\rm e}(t_k) - h_{\rm e}(\hat{\mathbf{x}}_{\rm e}^-)), \tag{8}$$

$$\hat{\mathbf{x}}_{\rm o}(t_k) = \hat{\mathbf{x}}_{\rm o}^- + K_{\rm o}(\mathbf{y}_{\rm o}(t_k) - h_{\rm o}(\hat{\mathbf{x}}_{\rm o}^-)), \tag{9}$$

$$P_{\rm e}(t_k) = (I_{(2)} - K_{\rm e}C_{\rm e})P_{\rm e}^-, \tag{10}$$

$$P_{\rm o}(t_k) = (I_{(2)} - K_{\rm o}C_{\rm o})P_{\rm o}^-. \tag{11}$$

where:

$$K_{\rm e} = P_{\rm e}^- C_{\rm e}^{\rm T}(C_{\rm e}P_{\rm e}^- C_{\rm e}^{\rm T} + R_{\rm e})^{-1}, \tag{12}$$

$$K_{\rm o} = P_{\rm o}^- C_{\rm o}^{\rm T}(C_{\rm o}P_{\rm o}^- C_{\rm o}^{\rm T} + R_{\rm o})^{-1}, \quad \text{and} \tag{13}$$

$$C_{\rm e} := \frac{\partial h_{\rm e}}{\partial \mathbf{x}_{\rm e}}^{\rm T} = \begin{bmatrix} \nabla^{\rm T}\mathbf{p}_{\rm e} & 0 \\ 0 & 1 \end{bmatrix}, \tag{14}$$

$$C_{\rm o} := \frac{\partial h_{\rm o}}{\partial \mathbf{x}_{\rm o}}^{\rm T} = \begin{bmatrix} \nabla^{\rm T}\mathbf{p}_{\rm o} & 0 \\ 0 & 1 \end{bmatrix}. \tag{15}$$

The true boresight angle, namely, the inclination of the line of sight from the ego car to the other car, measured in the $\mathcal{I}$-axes is given by:

$$\alpha_{\rm true}^{\rm I} := \tan^{-1}\left(\frac{p_{y,{\rm o}}(s_{\rm o}) - p_{y,{\rm e}}(s_{\rm e})}{p_{x,{\rm o}}(s_{\rm o}) - p_{x,{\rm e}}(s_{\rm e})}\right).$$

As the true values of the state $s_{\rm e}, s_{\rm o}$ are not available, the boresight angle used for beamforming is based on the estimated values, namely:

$$\alpha_{\rm est}^{\rm I} := \tan^{-1}\left(\frac{p_{y,{\rm o}}(\hat{s}_{\rm o}) - p_{y,{\rm e}}(\hat{s}_{\rm e})}{p_{x,{\rm o}}(\hat{s}_{\rm o}) - p_{x,{\rm e}}(\hat{s}_{\rm e})}\right).$$

IV. Numerical Simulation Experiments

For this paper, we consider two scenarios: (i) An intersection of two straight roads, and (ii) An intersection of a straight road with a roundabout. Both of these scenarios are shown in Fig. 2. The road definitions for the first scenario (straight road intersection) are:

$$\mathbf{p}_{\rm e}(0) = \begin{bmatrix} 525 \\ 0 \end{bmatrix} \text{ m}, \quad \mathbf{p}_{\rm e}(s_{\rm e}) = \mathbf{p}_{\rm e}(0) + s_{\rm e}\begin{bmatrix} \cos 70^\circ \\ \sin 70^\circ \end{bmatrix},$$

$$\mathbf{p}_{\rm o}(0) = \begin{bmatrix} 0 \\ 450 \end{bmatrix} \text{ m}, \quad \mathbf{p}_{\rm o}(s_{\rm o}) = \mathbf{p}_{\rm o}(0) + s_{\rm o}\begin{bmatrix} 1 \\ 0 \end{bmatrix},$$

while the road definitions in the second scenario (roundabout) are given by:

$$\mathbf{p}_{\rm e}(0) = \begin{bmatrix} 100 \\ 0 \end{bmatrix} \text{ m}, \qquad \mathbf{p}_{\rm e}(s_{\rm e}) = \mathbf{p}_{\rm e}(0) + s_{\rm e}\begin{bmatrix} 0 \\ 1 \end{bmatrix}$$

$$\mathbf{p}_{\rm o}(s_{\rm o}) = \begin{bmatrix} 100 \\ 285 \end{bmatrix} + \rho\begin{bmatrix} \cos(\frac{s_{\rm o}}{\rho} + \theta_0) \\ \sin(\frac{s_{\rm o}}{\rho} + \theta_0) \end{bmatrix} \text{ m},$$

where $\rho := 100$ m and $\theta := \frac{\pi}{2}$.

[2]For two successive ego car self-localization measurements, $\delta t = \delta t_{\rm e}$.

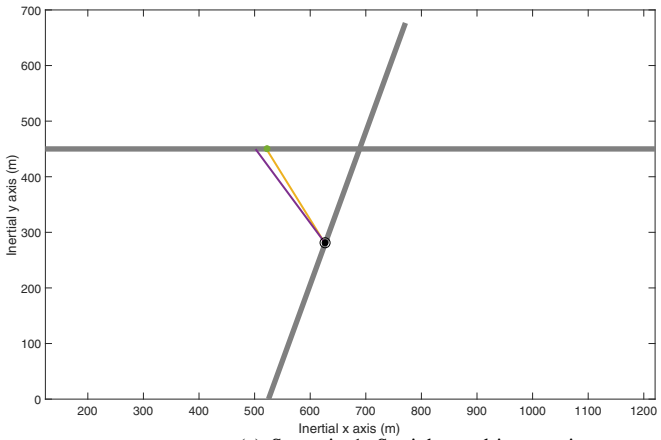

(a) Scenario 1: Straight road intersection.

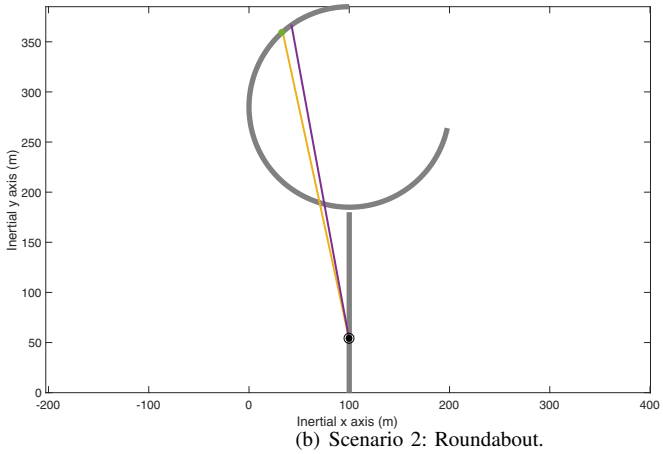

(b) Scenario 2: Roundabout.

Fig. 2. A scale drawing of the road scenarios considered for numerical experiments. The encircled black dot represents the ego car, whereas the green dot represents the other car. The yellow line illustrates, at a particular time instant, the estimated boresight, whereas the purple line indicates boresight calculated using measurements and communicated data alone (*i.e.*, without the proposed estimation scheme).

In both scenarios, the noise characteristics are the same, namely:

$$q_{\mathrm{e}} = q_{\mathrm{o}} = 6.25 \times 10^{-4}\ \mathrm{m}^2/\mathrm{s}^4,$$
$$R_{\mathrm{e}} = \mathrm{diag}(0.25\ \mathrm{m}^2, 0.25\ \mathrm{m}^2, 0.0625\ \mathrm{m}^2/\mathrm{s}^2),$$
$$R_{\mathrm{o}} = \mathrm{diag}(36\ \mathrm{m}^2, 36\ \mathrm{m}^2, 0.0625\ \mathrm{m}^2/\mathrm{s}^2).$$

The results with respect to improvements in boresight angle estimation are presented next. To this end, we first compare the estimated boresight angle $\alpha^{\mathrm{I}}_{\mathrm{est}}$ to its true value $\alpha^{\mathrm{I}}_{\mathrm{true}}$. We also compare the difference between the estimated boresight angle and the boresight angle that can be computed from the measurements and V2V communications alone. Specifically, this angle is defined by:

$$\alpha^{\mathrm{I}}_{\mathrm{meas}} := \tan^{-1}\left(\frac{\mathbf{y}_{\mathrm{o},2} - \mathbf{y}_{\mathrm{e},2}}{\mathbf{y}_{\mathrm{o},1} - \mathbf{y}_{\mathrm{e},1}}\right),$$

where, *e.g.*, $\mathbf{y}_{\mathrm{e},1}$ indicates the first element of the vector $\mathbf{y}_{\mathrm{e}}$.

Fig. 3 shows the comparison of these three angles for the straight intersection scenario. Fig. 3(b) shows the absolute

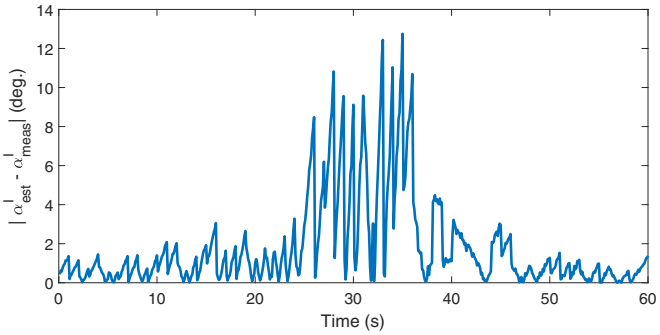

Fig. 3. Comparison of true, estimated, and measured boresight angles from the transmitter for the straight-line intersection road scenario.

difference $|\alpha^{\mathrm{I}}_{\mathrm{est}} - \alpha^{\mathrm{I}}_{\mathrm{meas}}|$. Informally, this absolute difference is an improvement in boresight estimation due to the proposed estimation scheme, without which we would have to use $\alpha^{\mathrm{I}}_{\mathrm{meas}}$ or $\alpha^{\mathrm{E}}_{\mathrm{meas}}$ as the reference angle for beamforming. Fig. 5 provides similar plots for the roundabout scenario, where the absolute difference $|\alpha^{\mathrm{I}}_{\mathrm{est}} - \alpha^{\mathrm{I}}_{\mathrm{meas}}|$ is observed to be even larger.

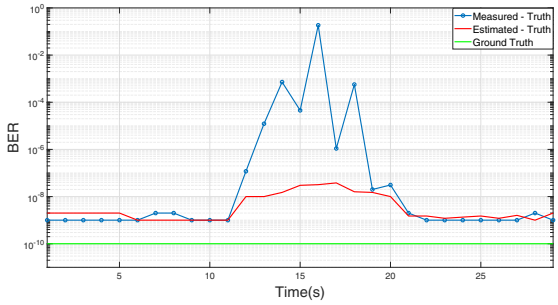

Fig. 4. BER results representing ground truth as the frame of reference and the difference between the measured and truth and the estimated and truth are plotted for straight-line intersection scenario.

Fig. 4 describes the Bit Error Rate (BER) with respect to time in seconds for the straight road intersection scenario. For the receiver, with its maximum positional error displacement from the transmitter, we observe that when beamforming is employed the losses are found to increase. On the other hand, if the estimated location of the vehicles calculated from the proposed state estimation model are known, the bits lost are not as high when compared with the measured error location of the vehicle. From Fig. 4, when the dual beamforming is employed between the transmitter and the estimated location of the receiver, the BER significantly increases, resulting in a beam lock that enhances the wireless communications between the two vehicles.

Fig. 6 illustrates the BER with respect to time in seconds for the roundabout road scenario. Similar to the aforementioned case, the maximum angular displacement between the error location of the vehicle and the transmitter was around 48° while for the estimated location of the vehicle and the transmitter, this displacement was measured to be equal to 15°. From Fig. 6, the beampatterns formed between time

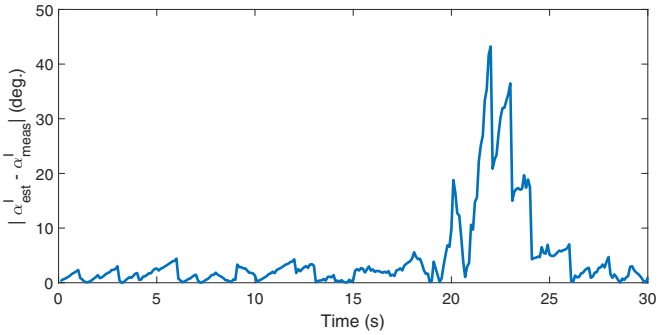

Fig. 5. Comparison of true, estimated, and measured boresight angles for the roundabout scenario.

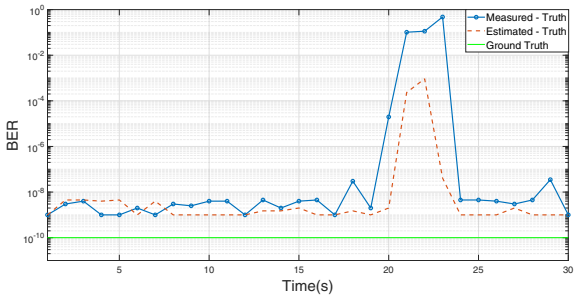

Fig. 6. BER results illustrating the difference in the measured and truth angles and the estimated and truth angles with ground value as the frame of reference for the roundabout case.

instants $19(s)$ to $24(s)$ yield a BER value for vehicle's error location that significantly decrease when compared to the vehicle's estimated location. In both road case scenarios, having the beampatterns pointed at the estimated position obtained from the proposed state estimation model yields improved communications between the transmitter and the receiver when compared with the error location information of the vehicle.

V. Conclusion

We present a state estimation model for mitigating positioning errors employing dual beamforming and obtain performance characteristics that were evaluated using MATLAB simulations for straight-line intersection and roundabout case scenarios. The results show that using this approach, it significantly mitigates the error in estimating the vehicle's location and achieves perfect beam lock when compared to the location information of the vehicle obtained from the overhead channels. Using Kalman filtering techniques when the locations of the receiver are estimated, the BER significantly increases when compared to the error locations of the vehicle occurring since the variations in the delays are due to overhead channels or GPS errors in the vehicular networks.

VI. Acknowledgement

The authors would like to sincerely thank the generous support from the US National Science Foundation (NSF) for their support of these research activities (Award Number CPS-1646367).

References

[1] J. Levinson, J. Askeland, J. Becker, J. Dolson, D. Held, S. Kammel, J. Z. Kolter, D. Langer, O. Pink, V. Pratt, M. Sokolsky, G. Stanek, D. Stavens, A. Teichman, M. Werling, and S. Thrun, "Towards fully autonomous driving: Systems and algorithms," in *2011 IEEE Intelligent Vehicles Symposium (IV)*, June 2011, pp. 163–168.

[2] I. R. S. Ruiz, D. Aufderheide, and U. Witkowski, "Radar sensor implementation into a small autonomous vehicle," in *Advances in Autonomous Mini Robots*, U. Rückert, S. Joaquin, and W. Felix, Eds. Berlin, Heidelberg: Springer Berlin Heidelberg, 2012, pp. 123–132.

[3] T. Wang, J. Xin, and N. Zheng, "A method integrating human visual attention and consciousness of radar and vision fusion for autonomous vehicle navigation," in *2011 IEEE Fourth International Conference on Space Mission Challenges for Information Technology*, Aug 2011, pp. 192–197.

[4] Google maps API documentation.

[5] OpenStreetMap contributors, "Planet dump retrieved from https://planet.osm.org ," https://www.openstreetmap.org, 2017.

[6] J. Wei, J. M. Snider, J. Kim, J. M. Dolan, R. Rajkumar, and B. Litkouhi, "Towards a viable autonomous driving research platform," in *2013 IEEE Intelligent Vehicles Symposium (IV)*, June 2013, pp. 763–770.

[7] B. Aygun, C. W. Lin, S. Shiraishi, and A. M. Wyglinski, "Selective message relaying for multi-hopping vehicular networks," in *2016 IEEE Vehicular Networking Conference (VNC)*, Dec 2016, pp. 1–8.

[8] B. Aygun and A. M. Wyglinski, "A voting-based distributed cooperative spectrum sensing strategy for connected vehicles," *IEEE Transactions on Vehicular Technology*, vol. 66, no. 6, pp. 5109–5121, June 2017.

[9] Y. Chen, Z. Xiang, W. Jian, and W. Jiang, "A cross-layer aomdv routing protocol for v2v communication in urban vanet," in *2009 Fifth International Conference on Mobile Ad-hoc and Sensor Networks*, Dec 2009, pp. 353–359.

[10] D. Lin, J. Kang, A. Squicciarini, Y. Wu, S. Gurung, and O. Tonguz, "Mozo: A moving zone based routing protocol using pure v2v communication in vanets," *IEEE Transactions on Mobile Computing*, vol. 16, no. 5, pp. 1357–1370, May 2017.

[11] S. Pagadarai, A. M. Wyglinski, and R. Vuyyuru, "Characterization of vacant uhf tv channels for vehicular dynamic spectrum access," in *2009 IEEE Vehicular Networking Conference (VNC)*, Oct 2009, pp. 1–8.

[12] D. Jiang, S. Li, Y. Wang, and J. Chen, "A channel allocation strategy for multi-hop cognitive radio networks," in *2013 Wireless Telecommunications Symposium (WTS)*, April 2013, pp. 1–6.

[13] D. Choudhury, "5g wireless and millimeter wave technology evolution: An overview," in *2015 IEEE MTT-S International Microwave Symposium*, May 2015, pp. 1–4.

[14] C.-T. Chen, *Linear System Theory and Design*, 3rd ed. New York, NY, USA: Oxford University Press, Inc., 1998.

[15] R. F. Stengel, *Optimal control and estimation*. Courier Corporation, 1986.